

A Colorful look at Climate Sensitivity

Bjorn Stevens¹ and Lukas Klufft¹

¹Max Planck Institute for Meteorology, Hamburg

Correspondence: Bjorn Stevens (bjorn.stevens@mpimet.mpg.de)

Abstract. The radiative response to warming, and to changing concentrations of CO₂, is studied in spectral space. If relative humidity does not change with temperature, clear-sky emissions over spectral intervals in which water vapor is optically thick become independent of surface temperature, giving rise to the idea of spectral masking. It is demonstrated that this idea allows one to derive simple, physically informative, and surprisingly accurate, expressions for the clear sky radiative forcing, radiative response to warming and hence climate sensitivity. Extending these concepts to include the effects of clouds, leads to the expectation that (i) clouds damp the clear-sky response to forcing, (ii) that diminutive clouds near the surface, which are often thought to be unimportant, may be effective at enhancing the clear-sky sensitivity over deep moist tropical boundary layers; (iii) even small changes in high-clouds over deep moist regions in the tropics make these regions radiatively more responsive to warming than previously believed; and (iv) cloud masking may contribute substantially to polar amplification. The analysis demonstrates that the net effect of clouds on warming is ambiguous, justifying the assertion that the clear-sky (fixed RH) climate sensitivity – which after accounting for clear-sky surface albedo feedbacks, is about 3 K – provides a reasonable prior for Bayesian updates accounting for how clouds are distributed, how they they might change, and for deviations associated with changes in relative humidity with temperature. These effects are best assessed by quantifying the distribution of clouds and water vapor, and how they change, in temperature, rather than geographic, space.

1 Introduction

In recent years, conceptualizing the effects of thermal infrared radiation in spectral space has helped advance understanding of many basic aspects of Earth's energy balance and how it responds to forcing. For instance, a consideration of the differential spectral response of outgoing long-wave radiation (OLR) to warming has proved crucial to understanding why OLR varies approximately linearly with temperature (Koll and Cronin, 2018), and how clear-sky radiative cooling is distributed through the depth of the troposphere (Jeevanjee and Fueglistaler, 2020; Hartmann et al., 2022). A spectral treatment of thermal-infrared radiation is also necessary to understand how radiation responds to forcing – in the form of increasing concentrations of atmospheric CO₂ (Wilson and Gea-Banacloche, 2012; Seeley, 2018; Jeevanjee et al., 2021b), and how it maintains an ability to respond to warming at very warm temperatures (Klufft et al., 2021; Seeley and Jeevanjee, 2021). Many of the above studies helped answer important questions by abandoning the idea that atmospheric radiative transfer could usefully be thought about as broadband, or grey. Grey atmospheres don't allow for spectral masking, which is a simple concept upon which much of the emergent understanding can be built.

In what follows, this more colorful way of thinking about radiative transfer is developed into a framework for thinking of climate sensitivity more broadly. We go about this by first demonstrating how a spectral view of radiative transfer, and in particular spectral masking (a concept defined more precisely below), helps quantify Earth's clear-sky climate sensitivity. While the concept of masking has a long history in radiative transfer, its application to irradiances at the top of the atmosphere provide a particularly effective heuristic for understanding how clouds and other trace-gases modify Earth's response to *forcing*¹, and how clouds, even with out changing, mediate Earth's response to *warming*. These ingredients demonstrate how, in addition to possible changes in cloud coverage, both the present-day distribution of clouds and their temperatures change with surface warming influence Earth's equilibrium climate sensitivity.

The ideas presented here were developed in lectures on the greenhouse effect the first author gave at the Universität Hamburg, in the Fall of 2021. Many had their origins in joint work with the second author. Subsequently we became aware that others were, or had been, thinking along similar lines, to understand cloud-free atmospheres. For instance, the simple model of CO₂ forcing discovered and presented in those lectures had been found independently, and much earlier, by Wilson and Gea-Banacloche (2012), and has since been elaborated upon further and more thoroughly by Seeley (2018), Jeevanjee et al. (2021b), and Romps et al. (2022). Likewise, the ideas related to the clear-sky radiative response were being developed independently by Jeevanjee et al. (2021a); McKim et al. (2021); Colman and Soden (2021); Koll et al. (2023). Given this literature, our study mostly ends up breaking new ground through its treatment of clouds, and hence its more overarching approach to the question of climate sensitivity. Because this builds on the concepts of masking (and unmasking) that we used to understand how clear-skies respond to forcing and to warming, it proves beneficial to retread what some readers might (now) consider as old ground, in our own way. In so doing we take care to point out in what way earlier (or contemporary) studies come to similar conclusions, with the added benefit that this allows us to present our ideas more concisely than would otherwise be possible.

The outline of the paper is as follows, after introducing the data sources and community tools used, the basic ideas behind spectral masking are introduced in §3, and used to derive estimates and provide understanding of Earth's clear-sky climate sensitivity and its components in §4. This provides a basis for thinking about Earth's equilibrium climate sensitivity more broadly (§5), and for better understanding the role of clouds in its determination. Conclusions and an outlook are presented in §6

2 Data

Absorption spectra of selective absorbers, here CO₂ and H₂O are taken from the catalog used for the Atmospheric Radiative Transfer Simulator, ARTS (Buehler et al., 2018; Eriksson et al., 2011). ARTS includes treatments of line broadening – with the treatment of the foreign-broadening appropriate for Earth's atmosphere, and a representation of continuum absorption following the approach of Clough et al. (1989, 2005) as modified by Mlawer et al. (2012). Other data sources include monthly mean, gridded (0.25° × 0.25°) near surface (2 m) air temperatures and column water vapor for the 240 months between 2001

¹Here forcing is used generically, for instance to refer to a change of atmospheric composition, and distinguished from *radiative forcing*, which is the response.

and 2021, and are taken from reanalyses of meteorological data (ERA5, Hersbach et al., 2019). Cloud data is based on measurements using the AATSR instrument which flew on ENVISAT (Poulsen et al., 2019). The record extends from May 60 2002 through April 2012 and level 3 cloud-top temperature and cloud fraction are used.

3 Theory

Concepts are developed for understanding the emission of terrestrial radiation, 99% of which is emitted in the 50 cm^{-1} to 2000 cm^{-1} wave-number interval, which is sometimes referred to as the long-wave or thermal infrared part of the electromagnetic spectrum. Earth’s atmosphere is assumed to consist of a background gas (dry-air) that is fully transparent to radiation emitted from its surface, absorption is limited to minor constituents, either particulate (clouds) which are assumed to be broad-band (colorless) absorbers, or by trace amounts of greenhouse gases (or vapors) which act as selective (or colorful) absorbers. A differentiation is made between short and long-lived greenhouse gases, whereby the phrase “short-lived” is short-hand for vapors, namely water vapor, which are assumed to exist in abundances (partial pressure) determined by the atmospheric temperature. Long-lived gases and vapors, like CO_2 , are well mixed, and assumed to be independent of the ambient temperature. 70 Scattering of terrestrial radiation is not considered. For the treatment of solar radiation clouds are treated as conservative scatterers, and gaseous absorption is neglected.

Our arguments are based on three simplifications:

S1 The effects of continuum absorption and line-broadening, while resolved spectrally, can be approximated by their values at an effective pressure, P (and in some cases temperature T , and composition) taken to be representative of the entire 75 column.

S2 The atmospheric relative humidity, \mathcal{R} is a fixed function of temperature, i.e., $\mathcal{R}(T)$.

S3 At a given wave-number, ν , *changes* in emission to space from a blackbody are assumed to be attenuated by the optical path above it.

S1 is mostly made for convenience, as it makes the physical arguments more transparent. Other studies, particularly Chou and 80 Kouvaris (1991) and more recently Romps et al. (2022) provide formal justification for this approach. In a somewhat stronger form (constant \mathcal{R}) the implication of **S2** was exploited by Nakajima et al. (1992); Ingram (2010); Goldblatt et al. (2013); Jeevanjee et al. (2021a), and in the earlier studies of runaway greenhouse atmospheres by Komabayasi (1967) and by Ingersoll (1969). **S3** differs from Beer’s law, which would normally be dismissed out of hand as it neglects the emission of the absorber, in that it refers to the *changes* in emission. It states, in a concise way, the basis for what we call masking, an idea that helps 85 conceptualize much of the recent literature on clear-sky radiative effects. While not a new idea, efforts to parameterize radiative transfer have long drawn on similar concepts, its use as a heuristic to understand factors influencing irradiances at the top of the atmosphere (troposphere) is shown to be particularly effective. **S2-S3** are elaborated upon in the remainder of this section, and their implications for understanding and quantifying Earth’s equilibrium climate sensitivity are explored in §4

3.1 Fixed relative humidity

90 3.1.1 Theory

The statement that the relative humidity, \mathcal{R} , does not change with warming (Arrhenius, 1896; Manabe and Wetherald, 1967) contains a subtle ambiguity. Is \mathcal{R} constant as a function of height, z , atmospheric pressure, P , or temperature T ? For a compressible atmosphere all three cannot be true. On physical grounds there is a reason to expect that \mathcal{R} is more constant with height in the lower troposphere (for instance the relative humidity over the sea-surface varies little over large ranges of temperature) and is more constant with temperature in the upper troposphere, which deepens with warming. **S2** adopts the latter description which implies that $P_v(T) = \mathcal{R}(T)P_*(T)$, where P_v and P_* denote the partial pressure of water vapor and its saturation value respectively.

Subject to weak restrictions on how T changes with P , a consequence of the above is that the water vapor burden,

$$W(z) = \int_z^{\infty} \rho_v dz \quad (1)$$

100 at some height z , with $\rho_v(z)$ the vapor density, is determined by the temperature, T , at that height alone. To demonstrate this we assume a hydrostatic atmosphere, $\rho g dz = -dP$, with ρ the total density of the air, and g the gravitational acceleration, and allow for a coordinate transform from $P \rightarrow T$ (which is equivalent to $P(T)$ being single valued). It follows that we can redefine W as

$$W(T) \approx \int_T^{T_{cp}} P_v(T') \left(\frac{R}{gR_v} \frac{d \ln(P(T'))}{dT'} \right) dT', \quad (2)$$

105 with R the mass specific gas constant of the air, and R_v the value for water vapor. The requirement that $P(T)$ be single valued is enforced by only considering contributions to W from heights below the cold-point tropopause², whose temperature is denoted by T_{cp} . The effect of this approximation is small, both by virtue of the smallness of $P_v(T_{cp})$ relative to its values at larger temperatures, and because we are mostly interested in $dW(T)/dT$, which is constrained by the smallness of differences in the mass of the stratosphere as the surface warms. Simulations suggests that T_{cp} is effectively constant across a wide range of conditions characteristic of the tropical atmosphere (Seeley et al., 2019). Hence we introduce it as a parameter, with the value $T_{cp} = 194 \text{ K}$ taken from radio occultation measurements in the tropics (Tegtmeier et al., 2020), bearing in mind that the same observations show substantially (20 K) larger values in the extra-tropics.

For the case whereby T follows an unsaturated adiabat, $\frac{d \ln(P)}{dT} = c_p/R$ and neglecting any co-variability of T with R_v , the specific heat of air, c_p , and the gravitational acceleration, g , results in

$$115 \quad W(T) \approx \frac{c_p}{gR_v} \int_T^{T_{cp}} P_v(T') dT'. \quad (3)$$

thereby articulating the conditions under which W is only a function of T , for a given $P_v(T)$.

²Here we are implicitly assuming that T can (notwithstanding near surface inversions) usefully be approximated as strictly decreasing in the troposphere

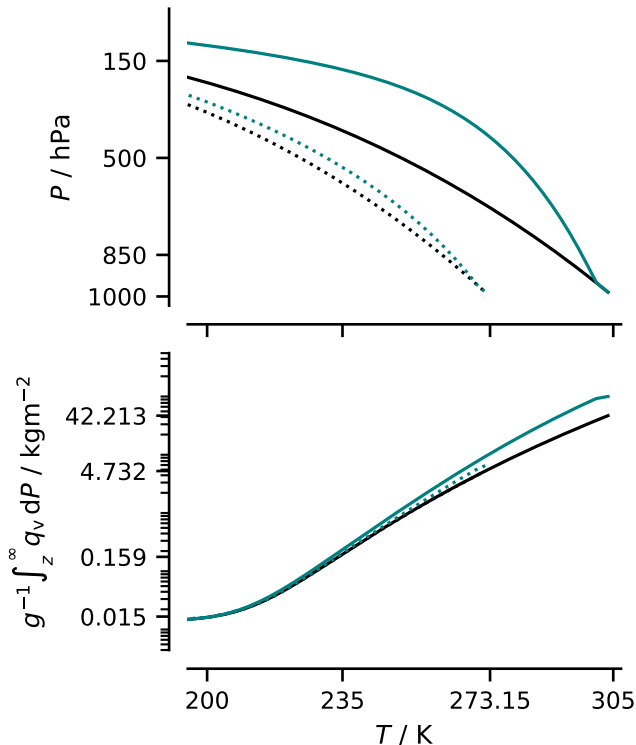


Figure 1. Theoretical temperature profiles and column humidities. Temperature profiles (left) following the formulation of the unsaturated (black) and saturated (teal) moist adiabats in Marquet and Stevens (2022) for two different surface temperatures (indicated). Column water vapor, $W(T)$, between the top of the atmosphere and the height corresponding to the indicated temperature (right).

The assumption that $d \ln(P)/dT$ depends only on T is better justified in the upper troposphere than in the middle and lower troposphere, where the temperature more closely follows the isentropic expansion of saturated air. The impact of allowing $d \ln(P)/dT$ to vary with P as it would following a saturated adiabat, is illustrated by Fig. 1, which compares values of $W(T)$ for temperature following saturated and unsaturated isentropic expansion. These have been calculated for $\mathcal{R} = \text{const.}$. Using a C-shaped profile of \mathcal{R} , as is more characteristic of the troposphere (Romps, 2014; Bourdin et al., 2021), albeit modified so the anchoring points depend on T , leads to similar conclusions. This then shows the extent to which the generality of our ideas is limited by variation of \mathcal{R} and $d \ln(P)/dT$ with P .

3.1.2 Observations

Across the Earth's surface it should come as no surprise that $P_v(T)$ varies from place to place, even if for any particular place it depends only on T . This gives rise to variations of W with T_{sfc} , which can be attributed to the effects of circulations. Because these circulations themselves co-vary with T_{sfc} they imprint themselves on the statistics of $W(T_{\text{sfc}})$. This can be seen by comparing $W(T_{\text{sfc}})$, as estimated from the the monthly averaged ERA5 data, with what would be expected for a fixed \mathcal{R} ,

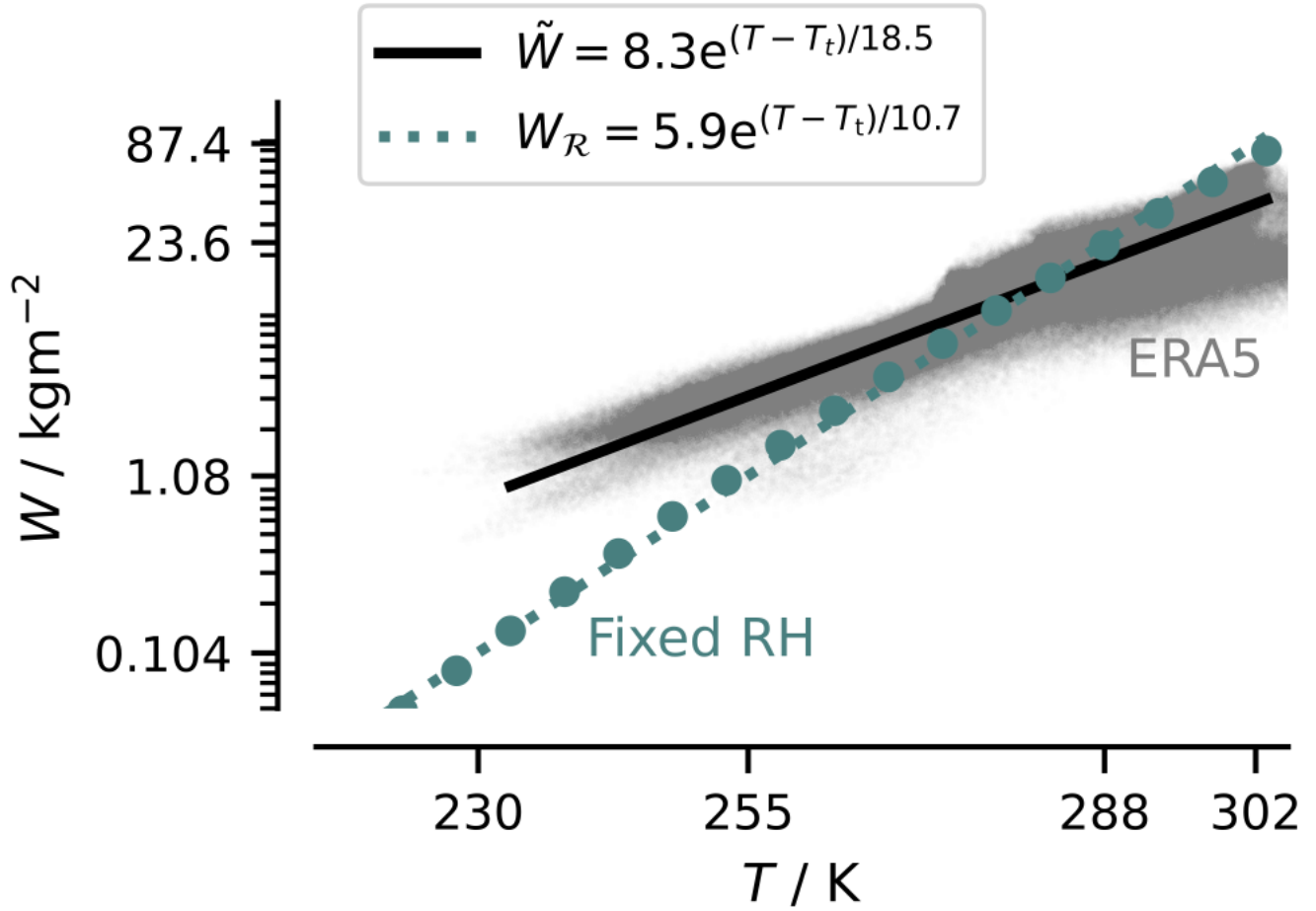


Figure 2. Column water vapor, W , versus T for $T = T_{\text{sfc}}$ and W given by the reanalysis (grey points) and for a fixed $\mathcal{R}(T)$ following an idealized C-shaped profile (filled teal-colored circles). The solid and dotted lines are fits whose slopes are chosen to match those of the grey and teal points respectively, with a crossing point at present-day global temperatures and are fit to the data by linearly regressing $\ln(W)$ binned by T against T .

which we denote by $W_{\mathcal{R}}$. W , binned by T_{sfc} , which we denote by \tilde{W} , still varies exponentially with T_{sfc} , just not as strongly
 130 as $W_{\mathcal{R}}$ varies with T . This difference is robust to how \mathcal{R} is specified, so long as it remains constant with T . C-shaped profiles
 yield a similar slope. The relative flatness of \tilde{W} expresses the fact that the cold extra-tropics have a higher water vapor burden
 at the surface, than does the warm tropical atmosphere above some height with the corresponding temperature – something
 familiar to those experiencing a winter day in Hamburg, compared to a summer day in the Alps at the same temperature. It
 also emphasizes an important distinction between $W_{\mathcal{R}}$ and \tilde{W} : whereas $W_{\mathcal{R}}$ portends to describe the water vapor burden at
 135 any temperature, irrespective of where it locates, \tilde{W} describes the water vapor burden that one would expect at the surface, on
 average, for the indicated surface temperature.

A consequence of the difference between $W_{\mathcal{R}}(T)$ and $\tilde{W}(T_{\text{sfc}})$ is that the former is more relevant to studying the effect
 of water-vapor on OLR across different climates, the latter for describing the spatial distribution of OLR and its scatter (cf
 Fig. 1 in Koll and Cronin (2018)) for a given climate. To the extent that the atmospheric circulation changes stays roughly
 140 constant with warming, one would expect the cloud of points, drawn from the distribution of atmospheric profiles, to shift
 following $W_{\mathcal{R}}$. For studies of the response of Earth’s atmosphere to warming, these findings motivate the rather simple choice
 of $\mathcal{R} = 0.8$, chosen so that $W_{\mathcal{R}}(T = \bar{T}_{\text{sfc}})$ matches $\tilde{W}(\bar{T}_{\text{sfc}})$. A relative humidity of 0.8 is larger than the mean \mathcal{R} , as it must
 be to capture the non-linearity of $W(T)$, whereby $\overline{W(T)} > W(\bar{T})$, with an over-bar denoting the global average.

3.2 Spectral masking

145 3.2.1 A Simpsonian atmosphere

We here review the implications of W depending only on T for the atmosphere’s optical properties. These ideas have a long
 history. Much of the modern literature follows the presentation of Ingram (2010) who, in developing a simple model for
 the water vapor feedback, recalled Simpson’s paradox (Simpson, 1928). While Ingram’s ideas have proven foundational for
 much of the recent literature, including this study, similar ideas were developed independently, and unbeknownst to Ingram, to
 150 study runaway greenhouse effects (Komabayasi, 1967; Ingersoll, 1969; Nakajima et al., 1992), albeit in ways that themselves
 appeared unaware of Simpson’s paradox. However one attributes it, the idea has proven so powerful that Jeevanjee et al. (2021a)
 went so far as to call it “Simpson’s Law”.

Assuming water vapor is the only important absorber, the optical depth of the atmosphere between a given height z and
 space is,

$$155 \quad \tau_{\nu}(z, \infty) = \int_z^{\infty} \kappa_{\nu, \nu} \rho_{\nu} dz \approx \kappa_{\nu} W(T(z)) \quad (4)$$

with $\kappa_{\nu, \nu}$ denoting the mass absorption cross section of water vapor at wave-number ν , at some effective (mass weighted)
 temperature and pressure, which follows from **S1**. This is Simpson’s Law, whereby $\tau_{\nu}(z)$ depends only on T at z .

As pointed out by Ingram (2010), the implication of the above is that at wavenumber ν and for W such that $\tau_{\nu, \nu} \gg 1$, surface
 emission is attenuated and atmospheric emissions become constant. At wavenumbers where $\tau_{\nu, \nu} \gg 1$, and by virtue of only
 160 depending on T , changing the temperature of the atmosphere only changes the effective height of the emission, not the amount.

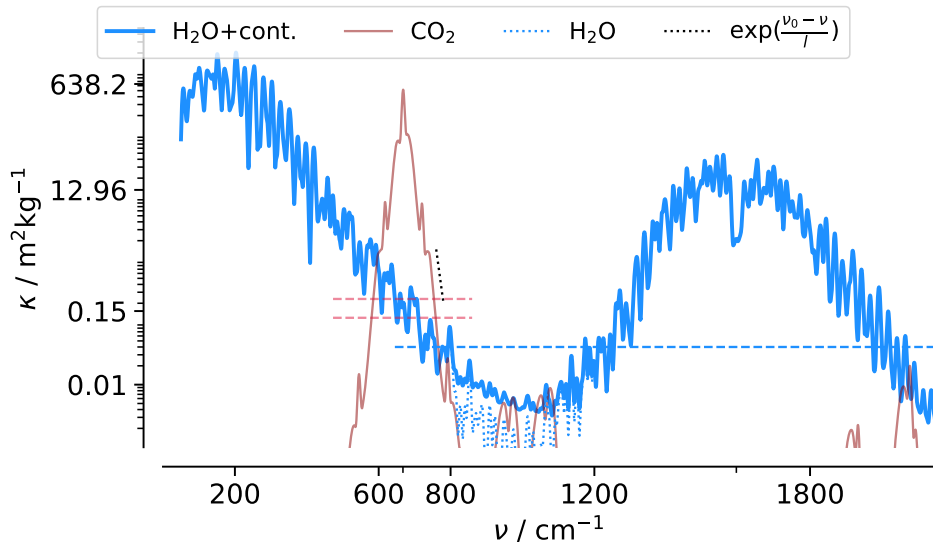


Figure 3. Mass absorption spectrum of H₂O (blue) and CO₂ (red) as a function of wave-number ν . Spectra are calculated at a wavenumber interval of 0.05 cm^{-1} for a temperature of 280 K and pressure of 850 hPa and smoothed by convolving with a Gaussian (9 cm^{-1}) filter to show the absorption envelope. For the dashed line envelope fit to the spectrum of CO₂, $l = 10.2 \text{ cm}^{-1}$.

This follows directly from Schwarzschild's equation (Chandrasekhar, 1960) for radiances, with the focusing more pronounced for gases or vapours that vary exponentially with temperature. It can (approximately) be extended to irradiances by taking an effective zenith angle, θ to scale the path length by $\mu^{-1} = (\cos \theta)^{-1}$ through the medium. The value of θ depends on the optical depth (Armstrong, 1968), but a value of $\theta = 53^\circ$ roughly corresponds to the average for optical depths uniformly distributed
165 between 0 and 1, resulting in the commonly adopted value of $\mu =^{-1} = 1.6$. For spectral regions where water vapor (or any absorber whose abundance is determined by T) controls the emission to space, i.e., $\mu^{-1} \tau_\nu > 1$, these emissions become invariant of T_{sfc} , something we refer to as spectral masking. This arises because, as T changes in physical space, the emitters simply redistribute themselves, retaining their abundances in temperature "space", and emit the same amount. It is the conceptual heart of the fixed relative humidity assumption and provides the justification for **S3**, which can thus be formulated as

$$170 \quad \delta F_\nu = \pi \left(e^{-(\tau_{\nu, \nu} / \mu)} \delta \mathcal{B}_\nu(T_{\text{sfc}}) \right), \quad (5)$$

with \mathcal{B}_ν the Planck source function. Further justification for Eq. 5 (equivalently **S3**) is provided by Jeevanjee et al. (2021a), whose analysis leads them to a broadband form (their Eq. (13)) of the same idea, which they call spectral cancellation. Eq. 5 can also be thought of as a generalization of the cooling to space approximation (Rodgers and Walshaw, 1966; Jeevanjee and Fueglistaler, 2020; Hartmann et al., 2022).

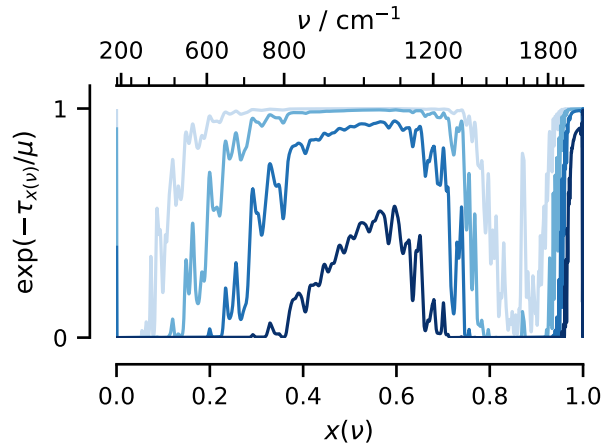


Figure 4. Spectral transmissivity plotted versus the cumulative black-body emission sensitivity, $x = (4\sigma T^3)^{-1} \int_0^\nu \left(\frac{dB_{\nu'}}{dT} \right) d\nu'$. The corresponding wave-numbers are indicated along the upper scale. Line colors darken with n for $W = 10^n \text{ kg m}^{-2}$ with $n = -1 \dots 2$.

175 3.2.2 The fractional support of the Planck response

Earth's globally averaged surface temperature is about 288 K and the average value of W is about 25 kg m^{-2} . When considering the spectrum of $\kappa_{\nu,\nu}$ (Fig. 3) it implies that $\forall \nu : \kappa_{\nu,\nu} \gg \bar{W}^{-1}$, $\tau_{\nu,\nu} \gg 1$. Modulo spectral smoothing hiding fine windows, this implies that the atmosphere is mostly opaque for $\nu < 800 \text{ cm}^{-1}$ or $\nu > 1200 \text{ cm}^{-1}$, which identifies the “atmospheric window” with the wave-number interval between these two limits. In that the radiative response to warming is carried by changing emissions at wave-numbers within this window, it can be said to define the “support” for this response

180

With the simplifications (S1–S3) we introduce the fractional support, χ . For a given $\tau_\nu(T) = \kappa_{\nu,\nu} W(T)$, it can be quantified as

$$\chi(T) = \frac{1}{4\sigma T^3} \int_0^\infty e^{-\frac{\tau_\nu(T)}{\mu}} \left(\frac{dB_\nu}{dT} \right) d\nu. \quad (6)$$

Koll and Cronin (2018) call the same quantity (their Eq. (4)) the average transmission. We adopt a different terminology because we associate the average transmission as being weighted by the Planck source function, not its derivative. The term “fractional support” is introduced to be more evocative of spectral masking, as it speaks to the idea of only a fraction of the wave-numbers participating in the Planckian response to warming.

185

The closing of the window with increasing W is manifest in $\chi(T)$ tending toward zero with increasing T as illustrated in Fig. 4. Here $e^{-(\kappa_\nu/\mu)W}$ has been plotted versus the fractional emission x , which is related to ν as

$$190 \quad dx = \frac{1}{4\sigma T^3} \left(\frac{dB_\nu}{dT} \right) d\nu \quad (7)$$

Choosing the x -axis in this manner stretches the ν axis so that equally spaced x intervals carry equal amounts of the radiative response. In terms of x , $\chi(T) = \int e^{-(\kappa_\nu/\mu)W} dx < 1$ is just the area under the curves in Fig. 4, which defines an effective

interval of x over which an emission response to changing temperatures is “supported” – hence the name. Fig. 4 also illustrates the difference between near line, versus continuum (or far-line/dimer), absorption. The former is associated with a narrowing of the window, while the latter is apparent by the reduction in χ within the window as W becomes large. Continuum emission is more broad-band and grey, whereas line-absorption, which more nearly results in $\chi(\nu) \in \{0, 1\}$, remains more colorful and better aligns with the concept of masking.

4 Spectral masking and climate sensitivity

Below we show how spectral masking can be used to understand the radiative response to both warming and to forcing. These are the two ingredients needed to understand the climate sensitivity of a constant albedo Simpsonian atmosphere, and how it is susceptible to the presence of clouds. We begin here with an application to the clear-sky atmosphere, which serves as a pre-requisite for our subsequent consideration of the effects of clouds in §5

4.1 Radiative response to warming

Assuming that the radiative response, δF , responds linearly to changes in T_{sfc} , we can write

$$\delta F = \lambda \delta T_{\text{sfc}}, \quad (8)$$

which introduces the proportionality constant, λ , as the radiative *response* parameter. It is closely related to the radiative *feedback* parameter, which is often denoted by the same symbol using the same expression, modulo a change in the sign convention to allow an increase in F with T to be associated with a negative value.

On the basis of **S1–S3**, the radiative response of a cloud-free Simpsonian atmosphere to the change in the temperature, T , of an underlying black-body may be written as

$$\Lambda(T) = \pi \int e^{-(\tau_{\nu, \nu}/\mu)} \left(\frac{dB_{\nu}}{dT} \right) d\nu = \chi(T) 4\sigma T^3, \quad (9)$$

We introduce Λ to distinguish the Simpsonian response to warming from the actual response, λ .

Modulo ambiguity in how W is defined in the expression for $\tau_{\nu, \nu}$, equivalently χ , Eq. (9) is identical to Eq. (3) in Koll and Cronin (2018). Applied to Earth this leads to the expectation that for a cloud-free (or clear-sky) atmosphere

$$\lambda \approx \Lambda(T_{\text{sfc}}) = \chi(T_{\text{sfc}}) 4\sigma T_{\text{sfc}}^3, \quad (10)$$

a quantity that is sometimes denoted as the clear-sky radiative response (or feedback), λ_{cs} .

Fig. 5 shows how χ varies with T , how this influences $\Lambda(T)$, and how both depend on the choice of $W(T)$. It is similar to Fig. 4 in Koll and Cronin (2018), which they calculated using slightly different assumptions.³ Whereas Koll and Cronin’s

³The degree of similitude can be ascertained by comparing the value of Λ where it maximizes (for the case of $W_{\mathcal{R}}$ and continuum absorption), which gives $2.50 \text{ W m}^{-2} \text{ K}^{-1}$ versus $2.43 \text{ W m}^{-2} \text{ K}^{-1}$ in Koll and Cronin, and its value at the low temperature limit which is (unchanged). The slightly smaller maximum in Koll and Cronin is consistent with their choice of $\mathcal{R} = 1$ versus $\mathcal{R} = 0.8$ in the present study

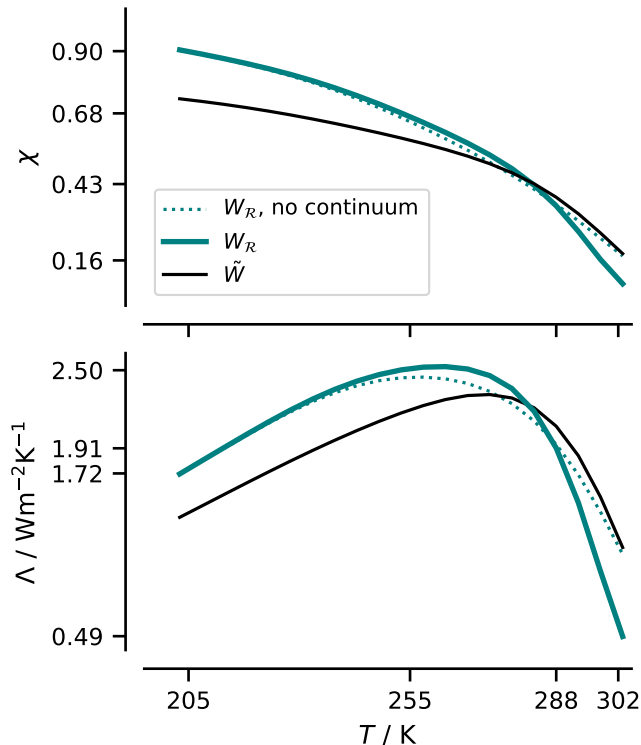


Figure 5. Variation of the support, $\chi(T)$, (upper) and the radiative response to warming, λ with T for different models of $W(T)$. Solid lines show calculations with the inclusion of continuum absorption the dotted line, for reference, shows the response in the absence of this absorption.

figure was presented in a way that emphasized the near constancy of Λ over the temperature range from 220 K to 280 K, our presentation emphasizes how much it varies, how this variation depends on the choice of W , and how it defines two temperature regimes. Roughly speaking, in the ice phase ($T < T_{\max}$), $d\Lambda/dT \approx 0.02 \text{ W m}^{-2} \text{ K}^{-2}$, while for a surface temperature supporting a liquid phase, $d\Lambda/dT \approx -0.1 \text{ W m}^{-2} \text{ K}^{-2}$.

The other point the figure makes is how accurate the simple estimates of $\lambda_{\text{cs}} \approx \Lambda(T_{\text{sfc}})$ end up being. For a global mean surface temperature of about 290 K, full radiative transfer calculations for an atmosphere in radiative convective equilibrium yield an estimate of $\lambda_{\text{cs}} = 2.2 \text{ W m}^{-2} \text{ K}^{-1}$ (McKim et al., 2021), as compared to $1.9 \text{ W m}^{-2} \text{ K}^{-1}$ in this study, with differences consistent with a larger choice of \mathcal{R} .

To the extent λ_{cs} can be usefully approximated by $\Lambda(T_{\text{sfc}})$, it demonstrates that this response is something that, given knowledge of the water vapor absorption spectra, is quite easy to understand. Essentially the reduction in λ_{cs} from what would be expected from a blackbody, measures how effective water vapor is at controlling emission to space, and thereby masking the spectral response of emissions to surface warming.

4.2 CO₂ radiative forcing

The concept of spectral masking, or rather unmasking, can be used to estimate the radiative forcing from a doubling of atmospheric CO₂, which we denote by δF . Here the CO₂ absorption feature around 667.5 cm⁻¹ masks emission from the lower troposphere (or surface) and increasing CO₂ increases the masking. Unlike for the case of water, for which the masked emissions don't change with warming, increasing the spectral footprint of CO₂, through a doubling of its concentration, leads to more of the near surface emissions being supplanted by emissions from the tropopause.

In the presence of CO₂ the OLR at the top of the atmosphere can be estimated by introducing the effective emission temperature at wavenumber ν , $T_{e,\nu}$, in the absence of CO₂, Jeevanjee et al. (2021b) adopt a similar approach. $T_{e,\nu}$ will depend on T_{sfc} in the window, and W elsewhere. At wavenumbers where CO₂ is strongly absorbing, emissions from within the troposphere are masked by those from the overlying atmosphere, which we take to be at the temperature T_{cp} . This choice of the CO₂ emission temperature effectively represents the stratosphere as isothermal, which finesses the problem of its adjustment to forcing Hansen et al. (1997). We construct the net emission by interpolating between the two limits using the CO₂ contribution to the transmissivity. This leads to a model of the form

$$F = \pi \int_0^{\infty} \left[e^{-(\tau_{\nu,c}/\mu)} \mathcal{B}_{\nu}(T_{e,\nu}) + \left(1 - e^{-(\tau_{\nu,c}/\mu)} \right) \mathcal{B}_{\nu}(T_{\text{cp}}) \right] d\nu. \quad (11)$$

Here $\tau_{\nu,c} \approx \kappa_{\nu,c}$ with $\kappa_{\nu,c}$, the mass absorption coefficient for CO₂ at wavenumber ν and C the CO₂ burden. Given this expression, the forcing from a doubling of atmospheric CO₂ becomes

$$\delta F = \pi \int_0^{\infty} \left(e^{-(\tau_{\nu,c}/\mu)} - e^{-2(\tau_{\nu,c}/\mu)} \right) [\mathcal{B}_{\nu}(T_{e,\nu}) - \mathcal{B}_{\nu}(T_{\text{cp}})] d\nu. \quad (12)$$

Because the difference between the exponential terms (CO₂ transmissivities) vanishes for $\tau_{\nu,c} \ll 1$ and for $\tau_{\nu,c} \gg 1$, $\mathcal{B}_{\nu}(T_{e,\nu})$ only contributes to the integral in the vicinity of the absorption feature. In this spectral range $T_{e,\nu} \approx \min(275, T_{\text{sfc}})$ as for $T_{\text{sfc}} > 275$ K water vapor becomes sufficiently abundant to mask the surface, and hence control emission (see e.g, Fig 8 in Jeevanjee et al. (2021b), and the CO₂ absorption spectrum in Fig. 3). With this simplification the forcing can be written as

$$\delta F = \pi \int_0^{\infty} \left(e^{-(\tau_{\nu,c}/\mu)} - e^{-2(\tau_{\nu,c}/\mu)} \right) [\mathcal{B}_{\nu}(\min(275, T_{\text{sfc}})) - \mathcal{B}_{\nu}(T_{\text{cp}})] d\nu. \quad (13)$$

For T_{cp} ranging from 194 K to 204 K (Tegtmeier et al., 2020), δF ranges from 4.3 W m⁻² to 3.9 W m⁻², in good agreement with the more elaborate calculations of Jeevanjee et al. (2021b), thereby demonstrating how δF can be rationalized on the basis of a relatively small number of assumptions (**S1-S3**).

4.3 Climate sensitivity

Combining the spectral masking based estimate of δF with the earlier estimate of λ_{cs} yields an estimate for the clear-sky climate sensitivity,

$$260 \quad \mathcal{S}_{\text{cs}} \equiv \frac{\delta F}{\lambda_{\text{cs}}} \approx \frac{4.3}{1.9} \approx 2.26 \text{ K}, \quad (14)$$

as compared to 2.1 K derived from radiative convective equilibrium calculations using full line-by-line radiative transfer.

Because CO_2 reclaims some of the spectrum from H_2O , it increases the fractional support of the response, increasing λ_{cs} relative to that of a CO_2 free atmosphere (Kluft et al., 2021; Seeley and Jeevanjee, 2021; Koll et al., 2023). This illustrates how the overlap between H_2O and CO_2 reduces \mathcal{S}_{cs} , both by reducing δF and by increasing λ_{cs} .

265 4.3.1 A simple expression for Earth's clear-sky climate sensitivity.

The physical content of Eq. (14) can be better illustrated by some simple approximations to the envelope of the absorption spectrum of water vapor and CO_2 , and its ability to mask spectral emission.

We first consider the radiative response to warming. By approximating $e^{-\tau_{\nu,\nu}}$ by unity outside, and zero inside, the atmospheric window, which based on Fig. 4 we take to be between 800 cm^{-1} to 1200 cm^{-1} , the Simpsonian response can be
 270 expressed simply as the integral of the response over the window,

$$\Lambda \approx \pi \int_{800}^{1200} \left(\frac{d\mathcal{B}_\nu}{dT} \right) d\nu. \quad (15)$$

Contributions from all other wavenumbers are masked by the Simpsonian response of water vapor. A similar conclusion was recently published by Colman and Soden (2021).

For the radiative forcing, Fig. 3 shows that the envelope of the CO_2 absorption spectrum falls off exponentially with ν as
 275 $\alpha e^{\|\nu - \nu_c\|/l}$, with $\nu_c = 667.5 \text{ cm}^{-1}$ denoting the line center. Wilson and Gea-Banacloche (2012) adopted this as a parameterization of the CO_2 spectrum, which implies that for a CO_2 burden of C , $\tau_{\nu,c} > 1$ for

$$\nu_c - l \ln(\alpha C) < \nu < \nu_c + l \ln(\alpha C). \quad (16)$$

From this expression, with $l \approx 10.2 \text{ cm}^{-1}$ as calculated by Jeevanjee et al. (2021b), it follows that for a burden of $2C$ the atmosphere becomes optically thick for the larger interval, larger by the amount $2l \ln(2)$. As \mathcal{B}_ν varies relatively slowly over
 280 the absorption band, $\mathcal{B}_\nu(T) \approx \mathcal{B}_{\nu_c}(T)$ over the interval where the difference between the CO_2 transmissivities in Eq. (13) appreciably departs from zero. With these simplifications the expression for the forcing simplifies to

$$\delta F \approx \pi 2l \ln(2) [\mathcal{B}_{\nu_c}(\min(275, T_{\text{sfc}})) - \mathcal{B}_{\nu_c}(T_{\text{cp}})], \quad (17)$$

similar to Eq. (14) in Jeevanjee et al. (2021b), who rigorously evaluate the arguments of Wilson and Gea-Banacloche (2012).

By incorporating the above simplifications, the clear-sky climate sensitivity can be expressed as

$$285 \quad \mathcal{S}_{\text{cs}} \approx 2l \ln(2) \frac{\mathcal{B}_{\nu_c}(\min(275, T_{\text{sfc}})) - \mathcal{B}_{\nu_c}(T_{\text{cp}})}{\int_{800}^{1200} \left(\frac{d\mathcal{B}_\nu}{dT} \right) d\nu} = 2.37 \text{ K}. \quad (18)$$

This estimate, which is derived from rather transparent reasoning, agrees well with calculation as given in Eq. (14), and with the detailed radiative transfer calculations by Kluff et al. (2019).

The main purpose of Eq. (18), is less about the quantitative fidelity of the arguments that brought us to it, as these are better addressed by other recent studies, e.g., Jeevanjee et al. (2021b, a); Romps et al. (2022) and Koll and Cronin (2018). Its main purpose is to demonstrate that a reasonable expectation for the clear sky climate sensitivity, and its dependence on quantities like surface temperature, forcing amount, and tropopause temperature, is quite easy to understand and that this provides a different way of thinking about cloud effects.

5 Inferences for Earth's atmosphere

Efforts to use the above ideas to understand the components of \mathcal{S}_{cs} , have, or are, also being developed simultaneously by other groups, as referenced above. Here we extend the scope of inquiry by exploring what they imply for the effects of clouds and for how temperature mediates the atmospheres radiative response to forcing (CO_2 changes) and to surface warming.

5.1 Cloud masking and unmasking

From the point of view of masking, what differentiates clouds from water vapor is that they are neither colorful, nor Simpsonian. Their first quality means that clouds will mask the forcing and the radiative response to warming, weakening both. When this is combined with their second quality, it raises the possibility that if clouds change their emission (to space) temperature with surface warming, they may unmask the spectral response otherwise masked by water vapor, and perhaps even enhance the radiative response to forcing.

While it is well known that clouds mask the radiative forcing (Myhre et al., 1998), this is sometimes overlooked when taking the measure of the cloud effect on climate sensitivity. The degree of masking will mostly depend on the cloud-top pressure, although a more minor effect might arise if clouds set a colder baseline than water vapor, i.e., lowering the approximate 275 K upper bound in Eq.(13). Focussing on the former, more dominant effect, an optically thick high-cloud fraction of $f_h = 25\%$, would reduce δF by the same amount, from 4.9 W m^{-2} (as calculated by Kluff et al., 2019) to 3.7 W m^{-2} . As a comparison, Myhre et al. (1998) estimate a similar, 27 %, reduction in CO_2 forcing due to clouds.

When the cloud-top emission-temperature, T_{cld} does not change with warming, clouds also mask window emissions in proportion to their (optically thick) cloud fraction (McKim et al., 2021). Given estimates of total cloud fraction, f_t , of about 0.6, this implies a commensurate reduction in λ , from $2.2 \text{ W m}^{-2} \text{ K}$ to $0.9 \text{ W m}^{-2} \text{ K}^{-1}$. Because all clouds, rather than just high clouds, contribute to the masking of emissions within the window, this effect is stronger than the reduction of the forcing, increasing \mathcal{S} by $(1 - f_h)/(1 - f_t) \approx 1.875$, raising \mathcal{S} to 4.2 K.

What seems to have escaped attention is how clouds might unmask parts of the spectrum otherwise masked by water vapor. To quantify these competing effects, we model the effects of clouds on λ as

$$\lambda \approx (1 - f) \Lambda_{\text{sfc}} + f \left(\frac{\delta T_{\text{cld}}}{\delta T_{\text{sfc}}} \right) \Lambda_{\text{cld}}, \quad (19)$$

which introduces Λ_x to denote $\Lambda(T_x)$ for reasons of notational convenience. The first term in Eq. (19), describes the masking of the clear-sky response (assuming $\lambda_{cs} \approx \Lambda_{sfc}$) by clouds, as earlier discussed by McKim et al. (2021), the second term describes the emission response across the spectrum as reclaimed, or unmasked, by clouds. Using this model we explore different limiting cloud effects below.

5.1.1 High clouds in the wet tropics

In the warm tropical atmosphere, where precipitating convection is embedded in a nearly saturated atmosphere (Bretherton and Peters, 2004), clouds may be especially important for the radiative response to warming. As the window closes, $\Lambda_{sfc} \rightarrow 0$, and there is nothing left for clouds to mask (Stephens et al., 2016). In this case the first term in Eq. (19) vanishes independent of f , clouds with cold cloud-tops will carry the entire radiative response, and its magnitude will be in proportion to the cloud fraction and the cloud-top temperature change. This would provide a thermostat for the tropical hothouse, one that is moderated by the effect of CO_2 which prevents the window from completely closing (Kluft et al., 2021; Seeley and Jeevanjee, 2021), and whose effectiveness will depend on the degree to which cloud-top temperature changes are constrained by the radiative cooling in the clear-sky atmosphere, which is still a matter of some debate (Zelinka and Hartmann, 2010, 2011; Bony et al., 2016; Seeley et al., 2019; Hartmann et al., 2022).

5.1.2 “Low clouds” coupled to surface temperature

In the case that clouds warm with the surface, $\delta T_{cld} \approx \delta T_{sfc}$, and $\lambda \approx \Lambda_{sfc} + f(\Lambda_{cld} - \Lambda_{sfc})$. In the warm regime Λ decreases with temperature, and because cloud-tops are colder than the surface, $\Lambda_{cld} - \Lambda_{sfc} > 0$. Candidate cloud regimes for such behavior would be clouds topping the trade-wind layer (Schulz et al., 2021), or clouds in the doldrums. In these cases one might expect $T_{sfc} - T_{cld} \approx 7 \text{ K}$ to 15 K , with surface temperatures increasingly exceeding 300 K . In this situation, from Fig. 5, clouds with tops at 288 K will radiate about three-fold more energy per degree of warming than would the surface. This is a bit misleading however, based on Fig. 3 of Koll and Cronin (2018) the aforementioned effect of CO_2 in maintaining emission to space, results in closer to 30% more energy per degree of warming. Nonetheless, this illustrates how shallow boundary layer clouds, even small ones that cover most of the tropical oceans but generally go unnoticed (Mieslinger et al., 2022; Konsta et al., 2022), may help stabilize the climate, albeit not as much as they would in the absence of CO_2 . Over the cold extra-tropics, where $\Lambda_{cld} - \Lambda_{sfc} < 0$, clouds have the opposite effect.

5.1.3 Open windows and multi-layer clouds

More generally, in the case where the window remains open ($\Lambda_{sfc} \neq 0$) and cloud masking limits the radiative response, the net effect of clouds will depend on $\delta T_{cld}/\delta T_{sfc}$. This can be more easily seen by rearranging Eq. (19):

$$\lambda \approx \Lambda_{sfc} \left[1 + f \left(\frac{\delta T_{cld}}{\delta T_{sfc}} \eta - 1 \right) \right], \quad \text{with} \quad \eta = \Lambda_{cld}/\Lambda_{sfc}. \quad (20)$$

In the cold regime clouds must warm more than the surface to offset their masking of window emissions. Over a warm surface more modest changes in cloud top temperatures may be sufficient to offset their masking effect, with the extreme case being that of high-clouds in the wet tropics.

This analysis can be generalized to clouds distributed over multiple layers, by working ones way down through the successive contribution of layers of non-overlapped clouds:

$$\lambda = \Lambda_{\text{sfc}} \left[1 + \sum_i f'_i \left(\frac{\delta T_{\text{cld},i}}{\delta T_{\text{sfc}}} \eta_i - 1 \right) \right] \quad (21)$$

where f'_i denotes the cloud fraction for layer i (increasing downward) that is not geographically masked by clouds at layers $j < i$.

5.1.4 Clouds and the clear-sky polar amplification paradox

From a purely radiative point of view, the idea that the polar latitudes should warm disproportionately is a curious one, as the radiative forcing from a doubling of atmospheric CO_2 is proportional to $T_{\text{sfc}} - T_{\text{cp}}$, which is much smaller in the polar regions, and the radiative response to warming is, by virtue of the absence of water vapor to mask surface emissions, particularly large. Put differently, from our understanding of the fixed albedo \mathcal{S}_{cs} , the tropics should warm substantially more than the poles as CO_2 increases. While this paradox might be resolved simply by considering surface albedo changes, clouds may also have a role to play.

To address this question more quantitatively we compare estimates of the \mathcal{S} with λ estimated following Eq. (19). We use $\tilde{W}(T_{\text{sfc}})$, rather than $W_{\mathcal{R}}$, to calculate Λ_{sfc} , and $W_{\mathcal{R}}$ is used to calculate Λ_{cld} . This is an admittedly crude way to treat the variation of W with height at different geographic regions, but using \tilde{W} for the cloud term as well does not change the answer appreciably. Clouds are represented using three bounding cases: (i) $f = 0$, which renders clouds as transparent; (ii) $\delta T_{\text{cld}} = \delta T_{\text{sfc}}$, whereby clouds warm with the surface; and (iii) $\delta T_{\text{cld}} = 0$, which describes Simpsonian clouds. To calculate δF requires an estimate of the forcing masking fraction f_{CO_2} , which we estimate based on the fractional decrease of the cloud-top temperature relative to the temperature change through the troposphere as a whole:

$$f_{\text{CO}_2} = \alpha \left(\frac{T_{\text{sfc}} - T_{\text{cld}}}{T_{\text{sfc}} - T_{\text{cp}}} \right) f_t. \quad (22)$$

with $\alpha = 1.9$ a tuning constant chosen so that $\overline{\delta F}$ matches the estimate of 3.7 W m^{-2} of more detailed calculations. Because \mathcal{S} is defined as a global (or statistical) quantity, it is estimated as $\overline{\delta F} / \overline{\lambda}$.

The results of these calculations are shown in Fig. 6. For case (i), with transparent clouds, $f = 0$, values of $\delta F / \lambda$ vary latitudinally from a low value (0.7 K) over the South Pole, to a high value (4.5 K) over the ITCZ region just north of the Equator, and thereby illustrating what we call the polar amplification paradox. For this case, $\mathcal{S} = 2.8 \text{ K}$ slightly larger than the clear-sky estimates obtained previously, using global mean quantities. The case (ii), with warming clouds ($\delta T_{\text{cld}} = \delta T_{\text{sfc}}$), $\mathcal{S} = 1.85 \text{ K}$ with reductions most pronounced in the tropics, where additional emissions from clouds occurs in an atmosphere that is less masked by water vapor. Given the idea that high-clouds maintain a fixed temperature, this case might seem extreme, then again,

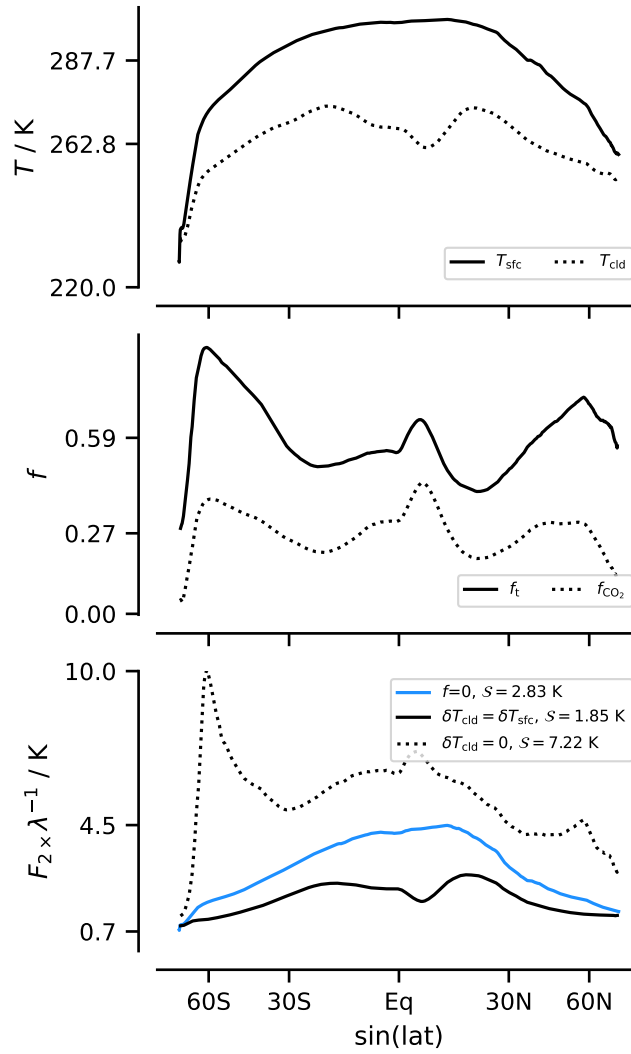


Figure 6. Latitudinal distribution of T_{sfc} and T_{cld} (upper), total cloud fraction f_t and fraction assumed to mask CO_2 forcing, δF (middle); and the ratio of the forcing δF to the radiative response to warming, λ for different assumptions about clouds (lower).

warming along the moist adiabat is upward amplified, so that the case of fixed cloud height actually implies $\delta T_{\text{cld}} > \delta T_{\text{sfc}}$, which can be thought of as a form of lapse-rate feedback. For case (iii), with $\delta T_{\text{cld}} = 0$, clouds mask the radiative response, and \mathcal{S} increases considerably, inverting its geographic structure to be more poleward amplified. This behavior depends on
380 f_{CO_2} , as for $f_{\text{CO}_2} = f$, the masking of the CO_2 forcing cancels the masking of the response and \mathcal{S} follows the transparent case.

5.1.5 Summarizing cloud effects on climate sensitivity

The above analysis identifies ways in which the amount and distribution of clouds influences the radiative response to warming, even if cloud coverage and temperatures do not change. A change in cloud top temperatures with warming can either increase or decrease the clear-sky climate sensitivity. This analysis also demonstrates that the role clouds plays can be quite different
385 in the cold extra-tropics versus the warm tropics, and that in addition to masking the forcing, there are a variety of additional ways in which clouds can reduce \mathcal{S} relative to \mathcal{S}_{cs} .

5.2 Discussion, and a proposal

To answer the question as to whether clouds increase or decrease Earth's equilibrium climate sensitivity we first ask how much clouds have to warm to compensate their masking effects. By adjusting δT_{cld} until $\mathcal{S} = \mathcal{S}_{\text{cs}}$ (which corresponds to the
390 transparent, $f = 0$, estimate in Fig. 6) we find that for $\delta T_{\text{cld}} \approx 1/2 \delta T_{\text{sfc}}$ the warming of clouds compensates their masking. Given that clouds also mask surface albedo changes with warming, whose assessed value of $0.35 \text{ W m}^{-2} \text{ K}^{-1}$ (Forster et al., 2021) is believed to be half of what it would be in a cloud-free atmosphere (Pistone et al., 2014), clouds only have to warm by about $1/4 \delta T_{\text{sfc}}$ to start having a net cooling effect relative to that expected from a clear sky, similar to what Kluft et al. (2019) estimate for the warming of high clouds in the tropics. Unless the amount of clouds change it seems that they make the system
395 less, rather than more, sensitive to forcing. To the extent that this assertion is at odds with conventional wisdom, this wisdom neither accounts for the ability of clouds to unmask the spectral response to warming, nor for their masking of the forcing. Even if cloud coverage does change, the assessed feedback from cloud amount changes is only $0.2 \text{ W m}^{-2} \text{ K}^{-1}$ (Forster et al., 2021), with recent work suggesting that it may be even smaller (Myers et al., 2021; Vogel et al., 2022). To balance this reduction in the radiative response would require clouds to warm on average by $\delta T_{\text{cld}} \approx 0.4 \delta T_{\text{sfc}}$. Based on these estimates, a null hypothesis
400 of no net cloud contribution to warming, but with a residual surface albedo feedback of $0.35 \text{ W m}^{-2} \text{ K}^{-1}$, doesn't seem far fetched – all the more so because it yields an estimate of \mathcal{S} of 2.96 K.

While this estimate does not fundamentally change our view on the value of climate sensitivity, that was not the point. Our ideas were never meant to replace detailed and accurate radiative transfer calculations, rather to find ways to think more physically about the factors that influence their results. Traditional feedback analysis adopts a grey perspective and attempts
405 to explain sources of differences in estimates of λ due to changes in quantities such as the lapse-rate, or in humidity. Our analysis shows how, irrespective of which humidity coordinate one adopts, this can be misleading. First because the lapse rate feedback is not physical: it is not changes in atmospheric temperature that influence emission, rather it is the redistribution of water, clouds or CO_2 with temperature that influence the emission; and second, because the distribution of clouds will mask

and unmask emissions from the surface or clouds, traditional feedback analysis risks conflating uncertainty from clouds as
410 uncertainty in non-cloud feedbacks.

To better link the contributions of the radiative response to the physics of radiant energy transfer, a different research programme is suggested. Such a programme would employ first-principle models of radiative transfer, and observations to:

1. quantify \mathcal{S}_{cs} as the clear-sky Simpsonian response to warming;
2. quantify “corrections” from unmasking by CO_2 and similar (albeit smaller) effects from other long-lived greenhouse
415 gases;
3. quantify “corrections” from cloud masking (Simpsonian clouds);
4. quantify “corrections” from: (i) non-Simpsonian clouds, (ii) non-Simpsonian water vapor; and (iii) changes to cloud coverage.

By beginning to address steps 2 and 4.ii Koll et al. (2023) take a step in this direction. One strength of the proposed programme
420 is that the first three steps can be constrained by theory and observations. Only the fourth step would require projections about future changes, or an extrapolation of past changes. If, in this, step the effects of clouds and relative humidity changes can be captured in terms of a few parameters, the method would lend itself well to Bayesian updating, which could also be used to help quantify uncertainty.

6 Conclusions

425 Assuming that the relative humidity, \mathcal{R} , does not vary with temperature, T , places a strong constraint on Earth’s radiative response to warming (Simpson, 1928; Nakajima et al., 1992; Ingram, 2010). In this limit, the radiative response to warming in those spectral intervals where water vapor is optically thick is nullified – something we call spectral masking. By accounting for this spectral masking it becomes straightforward to derive an expression (Eq.(9)) for Earth’s clear-sky radiative response to warming that is quantitatively and physically informative.

430 Spectral masking can also be extended to explain the effect of long-lived trace gases, which allows for simple expressions describing their radiative response to changes in their concentration, i.e., radiative forcing. With some further simplifications, following Wilson and Gea-Banacloche (2012), analytic expressions can be derived to describe the radiative forcing from changing concentrations of CO_2 , which when combined with the radiative response to warming yields an analytic expression, Eq. (14), for the clear-sky equilibrium climate sensitivity, \mathcal{S}_{cs} . These ideas help understand and quantify state dependence, i.e.,
435 \mathcal{S}_{cs} increasing with temperature (Caballero and Huber, 2013; Bloch-Johnson et al., 2021) – increasingly so for $T_{sfc} > 270\text{K}$ – and with humidity at a fixed temperature (Bourdin et al., 2021).

Spectral masking also provides a basis for thinking about how clouds modify \mathcal{S}_{cs} . Even for no change in geographic coverage, clouds can both mask emissions from the surface, and unmask emissions from the atmosphere below them. By virtue of locating at a different, usually colder, temperature than the surface, clouds that warm with the surface, amplify the radiative

440 response over a warm surface (making the system less sensitive), and damp the response over a cold surface (making the system more sensitive). Clouds thus introduce an thus additional state dependence to the climate sensitivity, one that depends on the temperature of the underlying surface, and their own emission temperature. This state dependence renders estimates of S sensitive to not just how clouds change, but also their base-state distribution. It also means that Earth's geographic tendency to have more clouds where it is colder moderates geographic variations in the ratio of the local radiative forcing to the local
445 radiative response, $\delta F/\lambda$, and may thereby be a source of the poleward amplification of warming.

Some surprising properties of clouds that emerge from this way of thinking are: (i) the potential of diminutive clouds in the tropics, whose cloud top temperatures are more closely bound to surface temperature changes, to increase the radiative response of the tropical atmosphere to warming; (ii) the importance of even small cloud-top temperature changes in regions of deep convection for amplifying the radiative response of the moist tropics to warming; (iii) the importance of cloud masking
450 at high-latitudes for increasing the sensitivity of regions whose clear-sky atmosphere would otherwise not be expected to be particularly susceptible to forcing. This highlights the many, albeit poorly quantified, ways by which clouds may reduce the climate sensitivity. Small changes in cloud-top temperatures, or in the amount of very thin low clouds atop the tropical boundary layer can compensate or compound changes in optically thick clouds. This renders the *net* cloud contribution to warming ambiguous, and adds weight to the value of a theoretical understanding of the clear-sky climate sensitivity and the
455 components which contribute to it.

The revised conceptual framework, combined with estimates of surface albedo feedbacks from the literature, allows us to quantify Earth's equilibrium climate sensitivity. The result, 3 K, doesn't meaningfully differ from values proposed by recent assessments adopting different approaches. However, our calculations outline an observational programme to determine this number more precisely through: (i) estimates from the historical record how \mathcal{R} is changing (cf Bourdin et al., 2021); (ii)
460 estimates of cloud masking by quantifying their present distribution; and (iii) estimates of how cloud changes are expected to change with warming (in coverage and temperature) based on observed trends and symmetries. By parameterizing these effects the method would be amenable to Bayesian updating and uncertainty quantification.

This study emphasizes how corrections to the clear-sky climate sensitivity of a planet with fixed albedo is determined by the temperature of its clouds, how this temperature differs from the temperature of the surface, and how it changes. Observations,
465 for instance by passive sensors sensitive to the most transparent parts of the spectrum or by active methods that can detect small and optically thin clouds (Wirth et al., 2009), that can help better quantify these corrections stand to advance understanding the most. Such measurements would help quantify the extent to which diminutive clouds, whose temperatures are coupled to the surface, strengthen the radiative response to warming, and by which high-clouds in cold regions, dampen it. Aligning the analysis of more complex models with the physics of the problem, e.g., by evaluating cloud responses in temperature and
470 wavenumber, rather than in physical space, offers opportunities for gleaning more insight as to the plausibility of the processes these models simulate, or parameterize, and the ultimate role of clouds in modifying Earth's clear-sky climate sensitivity.

Code availability. The code used to produce alll figurs and make all calculations is provides as a Python notebook on Zenodo

Author contributions. The presented concepts and ideas have been developed by BS and LK during a joint lecture. BS has performed the analysis, created the figures, and written the original draft, and its revisions based on comments raised by review. BS and LK have reviewed
475 and edited the submitted and revised manuscript.

Competing interests. We are not aware of any competing interests.

Acknowledgements. Manfred Brath helped with ARTS in the preparation and execution of the first author's greenhouse lectures. He and the developers of ARTS are thanked for their provision of such a useful community tool. Feedback from the students and participants at special seminars at ETH-Zurich, the University of Bern, CFMIP in Seattle, and at the 2022 CERES team meeting in Hamburg, where these ideas
480 were presented, is also acknowledged. Marty Singh helped clarify the first author's thinking on the Bayesian updating. Jean-Louis Dufresne is thanked for encouraging the development of these ideas. Two anonymous reviewers and the editor, Paolo Ceppi, are thanked for the time they spent in helping the author's clarify the presentation of their ideas. Nadir Jeevanjee and Daniel Koll who have helped pioneer the lines of reasoning we also follow, are thanked for helping the authors better anchor their ideas in the rapidly developing literature on this subject.

References

- 485 Armstrong, B.: Theory of the Diffusivity Factor for Atmospheric Radiation, *Journal of Quantitative Spectroscopy and Radiative Transfer*, 8, 1577–1599, [https://doi.org/10.1016/0022-4073\(68\)90052-6](https://doi.org/10.1016/0022-4073(68)90052-6), 1968.
- Arrhenius, S.: On the Influence of Carbonic Acid in the Air upon the Temperature of the Ground, *Philosophical Magazine Series 5*, 41, 237–276, 1896.
- Bloch-Johnson, J., Rugenstein, M., Stolpe, M. B., Rohrschneider, T., Zheng, Y., and Gregory, J. M.: Climate Sensitivity Increases Under Higher CO₂ Levels Due to Feedback Temperature Dependence, *Geophysical Research Letters*, 48, e2020GL089074, <https://doi.org/10.1029/2020GL089074>, 2021.
- 490 Bony, S., Stevens, B., Coppin, D., Becker, T., Reed, K. A., Voigt, A., and Medeiros, B.: Thermodynamic Control of Anvil Cloud Amount, *Proc Natl Acad Sci USA*, 113, 8927–8932, <https://doi.org/10.1073/pnas.1601472113>, 2016.
- Bourdin, S., Kluft, L., and Stevens, B.: Dependence of Climate Sensitivity on the Given Distribution of Relative Humidity, *Geophysical*
- 495 *Research Letters*, 48, e2021GL092462, <https://doi.org/10.1029/2021GL092462>, 2021.
- Bretherton, C. S. and Peters, M. E.: Relationships between Water Vapor Path and Precipitation over the Tropical Oceans, *Journal of Climate*, 17, 12, 2004.
- Buehler, S. A., Mendrok, J., Eriksson, P., Perrin, A., Larsson, R., and Lemke, O.: ARTS, the Atmospheric Radiative Transfer Simulator – Version 2.2, the Planetary Toolbox Edition, *Geoscientific Model Development*, 11, 1537–1556, [https://doi.org/10.5194/gmd-11-1537-](https://doi.org/10.5194/gmd-11-1537-2018)
- 500 2018, 2018.
- Caballero, R. and Huber, M.: State-Dependent Climate Sensitivity in Past Warm Climates and Its Implications for Future Climate Projections, *Proceedings of the National Academy of Sciences*, 110, 14 162–14 167, <https://doi.org/10.1073/pnas.1303365110>, 2013.
- Chandrasekhar, S.: *Radiative Transfer*, Dover, 1960.
- Chou, M.-D. and Kouvaris, L.: Calculations of Transmission Functions in the Infrared CO₂ and O₃ Bands, *Journal of Geophysical Research: Atmospheres*, 96, 9003–9012, <https://doi.org/10.1029/89JD00992>, 1991.
- 505 Clough, S., Kneizys, F., and Davies, R.: Line Shape and the Water Vapor Continuum, *Atmospheric Research*, 23, 229–241, [https://doi.org/10.1016/0169-8095\(89\)90020-3](https://doi.org/10.1016/0169-8095(89)90020-3), 1989.
- Clough, S., Shephard, M., Mlawer, E., Delamere, J., Iacono, M., Cady-Pereira, K., Boukabara, S., and Brown, P.: Atmospheric Radiative Transfer Modeling: A Summary of the AER Codes, *Journal of Quantitative Spectroscopy and Radiative Transfer*, 91, 233–244, <https://doi.org/10.1016/j.jqsrt.2004.05.058>, 2005.
- 510 Colman, R. and Soden, B. J.: Water Vapor and Lapse Rate Feedbacks in the Climate System, *Rev. Mod. Phys.*, 93, 045002, <https://doi.org/10.1103/RevModPhys.93.045002>, 2021.
- Eriksson, P., Buehler, S. A., Davis, C. P., Emde, C., and Lemke, O.: ARTS, the Atmospheric Radiative Transfer Simulator, Version 2, *Journal of Quantitative Spectroscopy and Radiative Transfer*, 112, 1551–1558, <https://doi.org/10.1016/j.jqsrt.2011.03.001>, 2011.
- 515 Forster, P., Storelvmo, T., Armour, K., Collins, W., Dufresne, J.-L., Frame, D., Lunt, D., Mauritsen, T., Palmer, M., Watanabe, M., Wild, M., and Zhang, H.: The Earth’s Energy Budget, Climate Feedbacks, and Climate Sensitivity, in: *Climate Change 2021: The Physical Science Basis. Contribution of Working Group I to the Sixth Assessment Report of the Intergovernmental Panel on Climate Change*, edited by Masson-Delmotte, V., Zhai, P., Pirani, A., Connors, S., Péan, C., Berger, S., Caud, N., Chen, Y., Goldfarb, L., Gomis, M., Huang, M., Leitzell, K., Lonnoy, E., Matthews, J., Maycock, T., Waterfield, T., Yelekeçi, O., Yu, R., and Zhou, B., p. 923–1054, Cambridge University
- 520 Press, Cambridge, United Kingdom and New York, NY, USA, <https://doi.org/10.1017/9781009157896.009>, 2021.

- Goldblatt, C., Robinson, T. D., Zahnle, K. J., and Crisp, D.: Low Simulated Radiation Limit for Runaway Greenhouse Climates, *Nature Geoscience*, 6, 661–667, <https://doi.org/10.1038/ngeo1892>, 2013.
- Hansen, J., Sato, M., and Ruedy, R.: Radiative Forcing and Climate Response, *J. Geophys. Res.*, 102, 6831–6864, <https://doi.org/10.1029/96JD03436>, 1997.
- 525 Hartmann, D. L., Dygert, B. D., Blossey, P. N., Fu, Q., and Sokol, A. B.: The Vertical Profile of Radiative Cooling and Lapse Rate in a Warming Climate, *Journal of Climate*, 35, 2653–2665, <https://doi.org/10.1175/JCLI-D-21-0861.1>, 2022.
- Hersbach, H., Bell, B., Berrisford, P., Biavati, G., Horányi, A., Muñoz Sabater, J., Nicolas, J., Peubey, C., Radu, R., Rozum, I., Schepers, D., Simmons, A., Soci, C., Dee, D., and Thépaut, J.-N.: ERA5 monthly averaged data on single levels from 1959 to present. Copernicus Climate Change Service (C3S) Climate Data Store (CDS). (Accessed on 12-Nov-2022), <https://doi.org/10.24381/cds.f17050d7>, 2019.
- 530 Ingersoll, A. P.: The Runaway Greenhouse: A History of Water on Venus, *Journal of Atmospheric Sciences*, 26, 1191–1198, [https://doi.org/10.1175/1520-0469\(1969\)026<1191:TRGAHO>2.0.CO;2](https://doi.org/10.1175/1520-0469(1969)026<1191:TRGAHO>2.0.CO;2), 1969.
- Ingram, W.: A Very Simple Model for the Water Vapour Feedback on Climate Change: A Simple Model for Water Vapour Feedback on Climate Change, *Q.J.R. Meteorol. Soc.*, 136, 30–40, <https://doi.org/10.1002/qj.546>, 2010.
- Jeevanjee, N. and Fueglistaler, S.: Simple Spectral Models for Atmospheric Radiative Cooling, *Journal of the Atmospheric Sciences*, 77, 479–497, <https://doi.org/10.1175/JAS-D-18-0347.1>, 2020.
- 535 Jeevanjee, N., Koll, D. D. B., and Lutsko, N.: “Simpson’s Law” and the Spectral Cancellation of Climate Feedbacks, *Geophysical Research Letters*, 48, e2021GL093699, <https://doi.org/10.1029/2021GL093699>, 2021a.
- Jeevanjee, N., Seeley, J. T., Paynter, D., and Fueglistaler, S.: An Analytical Model for Spatially Varying Clear-Sky CO₂ Forcing, *Journal of Climate*, 34, 9463–9480, <https://doi.org/10.1175/JCLI-D-19-0756.1>, 2021b.
- 540 Kluft, L., Dacie, S., Buehler, S. A., Schmidt, H., and Stevens, B.: Re-Examining the First Climate Models: Climate Sensitivity of a Modern Radiative–Convective Equilibrium Model, *Journal of Climate*, 32, 8111–8125, <https://doi.org/10.1175/JCLI-D-18-0774.1>, 2019.
- Kluft, L., Dacie, S., Brath, M., Buehler, S. A., and Stevens, B.: Temperature-Dependence of the Clear-Sky Feedback in Radiative-Convective Equilibrium, *Geophysical Research Letters*, 48, e2021GL094649, <https://doi.org/10.1029/2021GL094649>, 2021.
- Koll, D. D., Jeevanjeeb, N., and Lutsko, N. J.: An Analytical Model for the Clear-Sky Longwave Feedback, *Journal of Climate*, 35, submitted, 545 2023.
- Koll, D. D. B. and Cronin, T. W.: Earth’s Outgoing Longwave Radiation Linear Due to H₂O Greenhouse Effect, *Proc Natl Acad Sci USA*, 115, 10293–10298, <https://doi.org/10.1073/pnas.1809868115>, 2018.
- Komabayasi, M.: Discrete Equilibrium Temperatures of a Hypothetical Planet with the Atmosphere and the Hydrosphere of One Component-Two Phase System under Constant Solar Radiation, *Journal of the Meteorological Society of Japan. Ser. II*, 45, 137–139, 550 https://doi.org/10.2151/jmsj1965.45.1_137, 1967.
- Konsta, D., Dufresne, J.-L., Chepfer, H., Vial, J., Koshiro, T., Kawai, H., Bodas-Salcedo, A., Roehrig, R., Watanabe, M., and Ogura, T.: Low-Level Marine Tropical Clouds in Six CMIP6 Models Are Too Few, Too Bright but Also Too Compact and Too Homogeneous, *Geophysical Research Letters*, 49, e2021GL097593, <https://doi.org/10.1029/2021GL097593>, 2022.
- Manabe, S. and Wetherald, R. T.: Thermal Equilibrium of the Atmosphere with a Given Distribution of Relative Humidity, *Journal of Atmospheric Sciences*, 24, 241–259, [https://doi.org/10.1175/1520-0469\(1967\)024<0241:TEOTAW>2.0.CO;2](https://doi.org/10.1175/1520-0469(1967)024<0241:TEOTAW>2.0.CO;2), 1967.
- 555 Marquet, P. and Stevens, B.: On Moist Potential Temperatures and Their Ability to Characterize Differences in the Properties of Air Parcels, *Journal of the Atmospheric Sciences*, 79, 1089–1103, <https://doi.org/10.1175/JAS-D-21-0095.1>, 2022.

- McKim, B. A., Jeevanjee, N., and Vallis, G. K.: Joint Dependence of Longwave Feedback on Surface Temperature and Relative Humidity, *Geophysical Research Letters*, 48, e2021GL094074, <https://doi.org/10.1029/2021GL094074>, 2021.
- 560 Mieslinger, T., Stevens, B., Kölling, T., Brath, M., Wirth, M., and Buehler, S. A.: Optically Thin Clouds in the Trades, *Atmospheric Chemistry and Physics*, 22, 6879–6898, <https://doi.org/10.5194/acp-22-6879-2022>, 2022.
- Mlawer, E. J., Payne, V. H., Moncet, J.-L., Delamere, J. S., Alvarado, M. J., and Tobin, D. C.: Development and Recent Evaluation of the MT_CKD Model of Continuum Absorption, *Philosophical Transactions of the Royal Society A: Mathematical, Physical and Engineering Sciences*, 370, 2520–2556, <https://doi.org/10.1098/rsta.2011.0295>, 2012.
- 565 Myers, T. A., Scott, R. C., Zelinka, M. D., Klein, S. A., Norris, J. R., and Caldwell, P. M.: Observational Constraints on Low Cloud Feedback Reduce Uncertainty of Climate Sensitivity, *Nat. Clim. Chang.*, 11, 501–507, <https://doi.org/10.1038/s41558-021-01039-0>, 2021.
- Myhre, G., Highwood, E. J., Shine, K. P., and Stordal, F.: New Estimates of Radiative Forcing Due to Well Mixed Greenhouse Gases, *Geophys. Res. Lett.*, 25, 2715–2718, <https://doi.org/10.1029/98GL01908>, 1998.
- Nakajima, S., Hayashi, Y.-Y., and Abe, Y.: A Study on the ?Runaway Greenhouse Effect? With a One-Dimensional
570 Radiative?Convective Equilibrium Model, *Journal of Atmospheric Sciences*, 49, 2256–2266, [https://doi.org/10.1175/1520-0469\(1992\)049<2256:ASOTGE>2.0.CO;2](https://doi.org/10.1175/1520-0469(1992)049<2256:ASOTGE>2.0.CO;2), 1992.
- Pistone, K., Eisenman, I., and Ramanathan, V.: Observational Determination of Albedo Decrease Caused by Vanishing Arctic Sea Ice, *Proceedings of the National Academy of Sciences*, 111, 3322–3326, <https://doi.org/10.1073/pnas.1318201111>, 2014.
- Poulsen, C., McGarragh, G., Thomas, G., Stengel, M., Christensen, M., Povey, A., Proud, S., Carboni, E., Hollmann, R., and Grainger, D.:
575 ESA Cloud Climate Change Initiative (ESA Cloud_cci) data: Cloud_cci ATSR2-AATSR L3C/L3U CLD_PRODUCTS v3.0, Deutscher Wetterdienst (DWD) and Rutherford Appleton Laboratory (Dataset Producer), https://doi.org/10.5676/DWD/ESA_Cloud_cci/ATSR2-AATSR/V003, 2019.
- Rodgers, C. D. and Walshaw, C. D.: The Computation of Infra-Red Cooling Rate in Planetary Atmospheres, *Quarterly Journal of the Royal Meteorological Society*, 92, 67–92, <https://doi.org/10.1002/qj.49709239107>, 1966.
- 580 Romps, D. M.: An Analytical Model for Tropical Relative Humidity, *Journal of Climate*, 27, 7432–7449, <https://doi.org/10.1175/JCLI-D-14-00255.1>, 2014.
- Romps, D. M., Seeley, J. T., and Edman, J. P.: Why the Forcing from Carbon Dioxide Scales as the Logarithm of Its Concentration, *Journal of Climate*, 35, 4027–4047, <https://doi.org/10.1175/JCLI-D-21-0275.1>, 2022.
- Schulz, H., Eastman, R., and Stevens, B.: Characterization and Evolution of Organized Shallow Convection in the Downstream North Atlantic
585 Trades, *JGR Atmospheres*, 126, <https://doi.org/10.1029/2021JD034575>, 2021.
- Seeley, J. T.: Convection, Radiation, and Climate: Fundamental Mechanisms and Impacts of a Changing Atmosphere., Ph.D. thesis, University of California, Berkeley, CA, 2018.
- Seeley, J. T. and Jeevanjee, N.: H2O Windows and CO2 Radiator Fins: A Clear-Sky Explanation for the Peak in Equilibrium Climate Sensitivity, *Geophysical Research Letters*, 48, e2020GL089609, <https://doi.org/10.1029/2020GL089609>, 2021.
- 590 Seeley, J. T., Jeevanjee, N., and Romps, D. M.: FAT or FiTT: Are Anvil Clouds or the Tropopause Temperature Invariant?, *Geophys. Res. Lett.*, 46, 1842–1850, <https://doi.org/10.1029/2018GL080096>, 2019.
- Simpson, G. C.: Some Studies in Terrestrial Radiation, *Memoirs of the Royal Meteorological Society*, 2, 69–95, 1928.
- Stephens, G. L., Kahn, B. H., and Richardson, M.: The Super Greenhouse Effect in a Changing Climate, *Journal of Climate*, 29, 5469–5482, 2016.

- 595 Tegtmeier, S., Anstey, J., Davis, S., Dragani, R., Harada, Y., Ivanciu, I., Pilch Kedzierski, R., Krüger, K., Legras, B., Long, C., Wang, J. S., Wargan, K., and Wright, J. S.: Temperature and Tropopause Characteristics from Reanalyses Data in the Tropical Tropopause Layer, *Atmospheric Chemistry and Physics*, 20, 753–770, <https://doi.org/10.5194/acp-20-753-2020>, 2020.
- Vogel, R., Albright, A. L., Vial, J., Geet, G., Stevens, B., and Bony, S.: Strong Cloud–Circulation Coupling Explains Weak Trade Cumulus Feedback, *Nature*, <https://doi.org/10.1038/s41586-022-05364-y>, 2022.
- 600 Wilson, D. J. and Gea-Banacloche, J.: Simple Model to Estimate the Contribution of Atmospheric CO₂ to the Earth’s Greenhouse Effect, *American Journal of Physics*, 80, 306–315, <https://doi.org/10.1119/1.3681188>, 2012.
- Wirth, M., Fix, A., Mahnke, P., Schwarzer, H., Schrandt, F., and Ehret, G.: The Airborne Multi-Wavelength Water Vapor Differential Absorption Lidar WALES: System Design and Performance, *Appl. Phys. B*, 96, 201–213, <https://doi.org/10.1007/s00340-009-3365-7>, 2009.
- Zelinka, M. D. and Hartmann, D. L.: Why Is Longwave Cloud Feedback Positive?, *J. Geophys. Res.*, 115, D16 117, <https://doi.org/10.1029/2010JD013817>, 2010.
- 605 Zelinka, M. D. and Hartmann, D. L.: The Observed Sensitivity of High Clouds to Mean Surface Temperature Anomalies in the Tropics: Temperature Sensitivity of High Clouds, *J. Geophys. Res.*, 116, n/a–n/a, <https://doi.org/10.1029/2011JD016459>, 2011.